LAWRENCE
LIVERMORE
NATIONAL
LABORATORY

Measurement of cross sections for alpha-induced reactions on 197Au and thick-target yields for the ((alpha),(gamma)) process on 64Zn and 63Cu

M. S. Basunia, H. A. Shugart, A. R. Smith, E. B. Norman

January 5, 2007

Disclaimer

Measurement of cross sections for alpha-induced reactions on ^{197}Au and thick-target yields for the (α, γ) process on ^{64}Zn and ^{63}Cu

M. S. Basunia[1], H. A. Shugart[2], A. R. Smith[1], and E. B. Norman[3,4]

[1] *Nuclear Science Division, Lawrence Berkeley National Laboratory, Berkeley, California 94720, USA*
[2] *Department of Physics, UC Berkeley, Berkeley, California 94720, USA*
[3] *Lawrence Livermore National Laboratory, Livermore, California 94551, USA*
[4] *Department of Nuclear Engineering, UC Berkeley, Berkeley, California 94720, USA*

We have measured the cross sections for the ^{197}Au$(\alpha, \gamma)^{201}$Tl and ^{197}Au$(\alpha, 2n)^{199}$Tl reactions in the 17.9– to 23.9–MeV energy range, and ^{197}Au$(\alpha, n)^{200}$Tl reaction in the 13.4– to 23.9–MeV energy range using an activation technique. Thick-target yields for the ^{64}Zn$(\alpha, \gamma)^{68}$Ge (7– to 14–MeV) and ^{63}Cu$(\alpha, \gamma)^{67}$Ga (7–MeV) reactions were measured. For all measurements, natural elements were bombarded with He$^+$ beams from the 88″ Cyclotron at the Lawrence Berkeley National Laboratory (LBNL). Irradiated samples were counted using a γ-spectrometry system at LBNL's Low Background Facility. Measured ^{197}Au$(\alpha, \gamma)^{201}$Tl cross-sections were compared with the NON-SMOKER theoretical values. The thick-target yields for the ^{64}Zn$(\alpha, \gamma)^{68}$Ge and ^{63}Cu$(\alpha, \gamma)^{67}$Ga reactions are also compared with the theoretical yield, calculated numerically using the energy dependent NON-SMOKER cross section data. In both cases, measured values are found to follow a trend of overlapping the predicted value near the alpha nucleus barrier height and fall below with a slowly widening difference between them in the sub barrier energy points.

I. INTRODUCTION

Nucleosynthesis studies of elemental evolution in a stellar environment use an extensive network of nuclear reactions, of which cross section data for different nuclear reaction channels are important. Stable isotopes in the nuclear chart above iron are classified as *s*, *r*, and *p* nuclei depending upon their nucleosynthesis production processes. The *s*-isotopes are produced by the slow (*s*) neutron capture process in stellar environments of helium-burning, where beta decay usually occurs between subsequent captures of neutrons due to a moderate density of neutrons. The stable isotopes at the valley of

stability in the nuclear chart are considered as being produced through the *s*-process. On the other hand, the *r*-isotopes are produced in high density neutron environments resulting from explosive stars and are located in the neutron rich side in the nuclear chart. The *p*-isotopes, which are basically proton rich nuclei in the nuclear chart, have been identified to be produced through a sequence of photodisintegration processes starting from some preexisting seed nuclei [1]. During supernovae explosions, γ-rays are energetic enough to initiate subsequent neutron knock out through the (γ, *n*) reaction on the *s*- and *r*-processed seed nuclei. With the increased neutron separation energies in consecutive compound nuclei, competing (γ, *p*) and (γ,α) photodisintegration processes becomes important [2]. For experimental cross section measurements, however, the common practice is to measure the inverse reaction, for example (*p*,γ) or (α,γ), in the laboratory and to extract the cross section for the actual reaction of interest. Experimental data for these reactions in the astrophysical relevant energies, i.e. at the sub coulomb barrier interaction energies near the Gamov window, are very scarce. In recent years, some proton-capture cross sections in the mass range A=90-100 [3-5] and α-capture cross sections on ^{144}Sm, ^{70}Ge, ^{96}Ru, ^{112}Sn, and ^{63}Cu have been reported [6-10]. Most of the reported α–capture data are found to be 2 to 5 times lower than the Hauser-Feshbach statistical model predictions. Improved global α-optical model potentials were proposed [11] for improving the theoretical results at sub-barrier interaction energies and more experimental data for a wider target mass range are highly required [8]. A modified α-potential provided good agreement between the experimental and theoretical results for the ^{106}Cd(α,γ)^{110}Sn reaction cross sections, reported recently [12].

In addition to cross section data, thick-target yields are used for astrophysical thermonuclear reaction rate derivations [13,14], for studying the production of ^{26}Al$_{g.s.}$, ^{7}Be, ^{13}C, etc. [15-17], and also for cross section measurements [18,19]. At sub-coulomb barrier energies, where cross sections are usually very low, thick-target yield measurement provide useful data on various important nuclear reactions.

In the present work, cross section measurements for α-induced reactions on gold and thick-target yields for α capture reactions of ^{64}Zn and ^{63}Cu were measured. The ^{197}Au$(\alpha,\gamma)^{201}$Tl reaction cross section is reported in the 17.9-23.9 MeV energy range. The peak of the Gamow window for the ^{197}Au$(\alpha,\gamma)^{201}$Tl reaction at a p-process temperature T$_9$ = 3.0 (3×10^9 $^{\circ}$K) corresponds to lab α bombarding energy of 11.9–MeV with a width of 4.1–MeV. An earlier measurement by Necheva and Kolev [20] reported the upper limits for this reaction in the 11.2- to 35.9-MeV energy range because the signature gamma lines of ^{201}Tl decay were absent in their spectra. Other cross sections such as ^{197}Au$(\alpha,n)^{200}$Tl, and ^{197}Au$(\alpha,2n)^{199}$Tl are also measured and reported. Thick-target yields for the ^{64}Zn$(\alpha,\gamma)^{68}$Ge and ^{63}Cu$(\alpha,\gamma)^{67}$Ga reactions are measured in the energy range of 7- to 14-MeV and at 7 MeV energy, respectively, and are compared with the theoretical yield. The theoretical yield is computed numerically using the energy dependent NON-SMOKER cross-section data [21]. The peak and width of the Gamow windows for the ^{64}Zn$(\alpha,\gamma)^{68}$Ge and ^{63}Cu$(\alpha,\gamma)^{67}$Ga reactions at a p-process temperature T$_9$ = 3.0 correspond to lab α bombarding energies of 6.4 ± 3.1 and 6.3 ± 3.0 MeV, respectively. The α-nucleus coulomb barrier heights for ^{197}Au, ^{64}Zn, and ^{63}Cu are 21.1–, 9.9–, and 9.6–MeV, respectively.

II. EXPERIMENT

A. Target preparation and irradiation

Gold foils of thickness ~2 mg/cm^2 and 99.9% purity, used in this experiment, were purchased from Alfa Aesar, Ward Hill, Massachusetts, USA. Two 2.5 cm × 2.5 cm sheets were weighed using a precision balance of microgram range to determine the accurate foil thickness before making four targets out of each sheet. The foils were mounted on circular aluminum holders. Two stacks were prepared with each having four gold targets interspaced by three aluminum foils of thickness ~7 mg/cm^2. A titanium sheet of 0.016 inch thickness was placed at the end of each stack. The target stacks were mounted on a thick water-cooled copper block. The aluminum foils served as incident α-beam energy degraders and also as catchers for recoil nuclei from the gold foils to estimate the recoil fraction. The titanium sheet was used to measure the thick-target yield for the ^{48}Ti$(\alpha,n)^{51}$Cr reaction. The measured yield was used to verify the beam current integration by comparing our data with that from Ref. [14]. For determining the ^{64}Zn$(\alpha,\gamma)^{68}$Ge and ^{63}Cu$(\alpha,\gamma)^{67}$Ga reaction thick-target yields, natural zinc and copper targets of ~0.06 inch thickness were mounted on the copper block one at a time for irradiation.

Gold, zinc, and copper targets were bombarded with an α-beam (He$^+$) from the 88″ Cyclotron at Lawrence Berkeley National Laboratory (LBNL). The bombarding energy range for the gold foils was 13.6– to 24.0–MeV. Experimental data of beam current, irradiation time, and total integrated charge are presented in Table I. Exposed spots of about 3 mm diameter of the thin gold foil were found to be intact after the irradiation; only a slight burn color was visible. All foils along with the aluminum holders were placed and fixed carefully inside small circular plastic dishes for counting. The incident beam energy

on the successive target foils was determined based on the energy loss for the aluminum and gold foils using *dE/dx* values obtained using the TRIM (the transport of ions in matter) code [22]. The beam current was integrated in steps of 2-3 minutes during the irradiation using a Brookhaven Instruments Corporation Integrator output hooked to a multi-channel scalar. The system was calibrated with known current sources.

TABLE I. Some of the irradiation conditions of the Au, Zn, and Cu targets with He$^+$ beams.

Sample	Energy (MeV)	Current (~μA)	Irradiation time (hours)	Total charge ($\mu C \pm 5\%$)
Au stack	24.0 ± 0.3	1	6	20963
	18.0 ± 0.2	0.7	5	10221
Zn	14.0 ± 0.2	0.1	0.62	203
	10.0 ± 0.1	0.6	1	2158
	8.8 ± 0.1	1.5	2	10774
	7.9 ± 0.1	1.5	4	20783
	7.0 ± 0.1	1.8	7.08	33465
Cu	7.0 ± 0.1	1.4	1.25	6381

B. Data acquisition and analysis

Samples were counted with an HPGe detector immediately following the irradiation and later with another HPGe detector. The second HPGe detector was located at LBNL's Low Background Facility (LBF). The energy resolution of the LBF's HPGe detector was 1.9 keV (FWHM) at $E_\gamma = 1332.5$ keV and of 80% relative efficiency. The γ–ray energy spectra were accumulated in 16,384 channels using an ORTEC PC-based acquisition system. Partial γ–ray spectra collected at the LBF is shown in Fig. 1 for the characteristic 167-keV γ–ray from ^{201}Tl and 1077-keV from ^{68}Ga. The gold foil contained 99.9% gold, 0.03% silver, 0.05% copper, and a few other trace elements. The 171- and 184-keV γ–rays in Fig.1 appear from the ^{111}In and ^{67}Ga radioisotopes, respectively, that are produced mainly through the ^{109}Ag($\alpha,2n$)^{111}In and the ^{65}Cu($\alpha,2n$)^{67}Ga reaction channels. The ^{68}Ge radioisotope, produced through the ^{64}Zn(α,γ)^{68}Ge ($t_{1/2}=270.8\ d$) emits no γ–ray. It decays

to ^{68}Ga ($t_{1/2}=67.63\ min$), through electron capture (*EC*). The ^{68}Ga emits a 1077-keV γ–ray with an intensity of 3% through it's *EC*+β^+ decay to stable ^{68}Zn. Thus, the activity of ^{68}Ge was determined by measuring the γ–ray from the daughter ^{68}Ga activity under a secular equilibrium condition. Samples were counted at the detector surface for the signature γ–rays from the ^{201}Tl, ^{68}Ga and ^{67}Ga radioisotopes. For the ^{200}Tl and ^{199}Tl radioisotopes, γ–ray spectra at 12 cm from the detector surface were used for deducing the cross sections. The efficiency calibration of the HPGe detector for the surface, 12- and 25-cm positions was done following the same procedure described in Ref. [10].
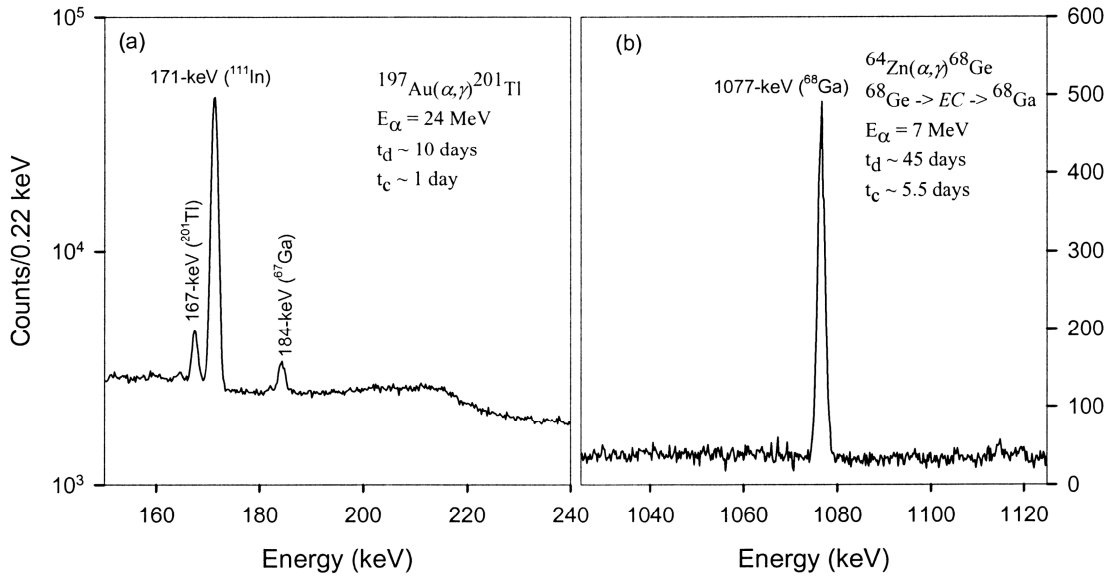

FIG. 1. Partial HPGe γ–ray spectra: (a) the 167–keV γ–ray from ^{201}Tl. ^{111}In and ^{67}Ga produced mainly through ^{109}Ag(α,2n)^{111}In and ^{65}Cu(α,2n)^{67}Ga reaction channels, and (b) the 1077-keV γ–ray from ^{68}Ga (t_d and t_c are cooling time and counting time, respectively).

All γ spectra were analyzed using ORTEC Gamma Vision software. The resolution of the HPGe detector was good enough to determine the 167-keV peak area conveniently, despite the strong presence of 171-keV γ–rays, as can be seen from Fig. 1. The cross sections were deduced from the well-known activation equation:

$$A_o = n\sigma\phi\left(1 - e^{-\lambda t}\right) \qquad (1)$$

Where, A_o = activity at the end of irradiation (disintegration/sec), n = number of target

nuclei (#/cm^2), σ = cross section (cm^2), ϕ = number of incident α particles per second

(#/sec), and $\left(1 - e^{-\lambda t}\right)$ = growth factor for a decay constant λ and irradiation time t.

The activity, A_o, at the end of irradiation was deduced from the measurement using the

following equation:

$$A_o = \lambda N_o = \lambda C \Big/ \left\{ I_\gamma \varepsilon \left(e^{-\lambda(t_{cs} - t_{ie})} - e^{-\lambda(t_{ce} - t_{ie})} \right) \right\} \qquad (2)$$

Where, N_o = number of product nuclei at the end of irradiation, t_{cs}, t_{ce}, t_{ie} = counting start,

counting end, and irradiation end times, respectively, C = total net count under the peak for

a counting duration $(t_{ce} - t_{cs})$, I_γ = absolute gamma ray intensity, and ε = detector peak

efficiency.

Based on equation (1), the thick-target yield, $Y(E)$, equation for a beam fully stopped in

the target is the following:

$$Y(E) = n \int_0^E \frac{\sigma(E')}{\left(-dE'/dx\right)} dE' = \frac{A_o}{\phi\left(1 - e^{-\lambda t}\right)} \qquad (3)$$

where E is the bombarding energy, $\sigma(E')$ is the energy dependent cross section, dE'/dx is

the stopping power, and the unit of n is (#/cm^3).

Nuclear data used to deduce the cross sections and the thick-target yields are presented

in Table II. For the gold stack irradiations, beam current measurement was done with a

calibrated source and by comparing the measured ^{48}Ti(α,n)^{51}Cr thick-target yields with the

experimental data from Ref. [14]. Similarly, for zinc and copper irradiations, the beam

current measurements were done comparing the measured thick-target yields for the

^{64}Zn(α,p)^{67}Ga and ^{65}Cu(α,n)^{68}Ga reactions, respectively, with the data from Ref. [14]. The data points of the thick-target yield of this experiment fall within the statistical limits on the trend line of reported data in Ref. [14]. The comparison shows a reliable current integration in this work.

TABLE II. Reaction and decay properties of the product radioisotopes [23].

Nuclear reaction	Half-life	E_γ (keV)	I_γ%
^{197}Au(α,γ)^{201}Tl	72.912 h ± 0.017	167.43	10.00 ± 0.06
^{197}Au(α,n)^{200}Tl	26.1 h ± 0.1	367.94	87.2 ± 0.4
^{197}Au($\alpha,2n$)^{199}Tl	7.42 h ± 0.08	208.2	12.3 ± 1.3*
^{64}Zn(α,γ)^{68}Ge	270.82 d ± 0.27	no γ	
$^{68}Ge\xrightarrow{\varepsilon+\beta^+}{}^{68}Ga$	67.629 min ± 0.024	1077.35	3.0 ± 0.3
^{63}Cu(α,γ)^{67}Ga	3.2612 d ± 0.0006	184.58	21.2 ± 0.3

*from *http://www.nndc.bnl.gov/nudat2/*

C. Sources of systematic uncertainty and correction factors

Uncertainties from target foil thickness, beam current, counting statistics, decay data, recoil fraction, detector efficiency calibration, and sample counting position, are considered in this work. Estimated contributions of the uncertainty from each category are tabulated in Table III and briefly discussed in the next paragraph. For thick-target yield measurements, sources of uncertainties from target thickness and recoil were inapplicable.

TABLE III. Sources of systematic uncertainty

Sources of uncertainty	Magnitude (%)
Foil thickness	3
Beam current	2
Net count	3-20
Decay data	~1, except $I\gamma$ (208) = 10.6
Recoiled fraction	1
Detector peak efficiency	5
HPGe surface counting position	~3

Uncertainty of the gold foil thickness was considered 2-3% that might arise due to non-uniformity of material throughout the foil sheet. The uncertainty from the beam current integration is estimated to be about 2% based on comparison of some measured experimental cross section data with the literature data as discussed in the previous section. In this work, cross sections were determined considering an averaged beam current using equation (1) and also using the differential equation of production and decay using the available current integration data from the multi scalar in steps of 2– or 3–minutes. Both averaged and differential beam current consideration produced exactly the same results. Only the ^{197}Au($\alpha,2n$)^{199}Tl reaction cross section at 17.9–MeV energy is reported using differential beam current, that is 3% lower than the result from average beam current consideration. The uncertainty associated with the net count of the peak of interest was found in the range of 3-20% in this work. The decay data of the radionuclides associate with the (α,γ) process were all below or around 1%. However, an uncertainty of 10.6% associated with the 208–keV γ-ray intensity, related to ^{197}Au($\alpha,2n$)^{199}Tl reaction, was considered in the uncertainty propagation. For determining the recoiled fraction, all aluminum foils were counted for γ–rays of the gold and thallium nuclei and that fraction was found to be between 3 and 5% using the ^{197}Au(α,n)^{200}Tl reaction. Assuming uniform recoil from all the gold foils, a 4% correction was made for each of the cross sections reported here. For efficiency calibration a 5% uncertainty is propagated considering standard calibration source strength uncertainty and other factors, like efficiency data points fitting curve, source size, etc. The selection of the surface counting position was essential to count the radioisotopes ^{201}Tl, ^{68}Ga and ^{67}Ga, produced through the (α,γ) process, for significant net counts under the peak of interest due to very weak activity. For

all of the above radionuclides the strongest γ-*ray* were used for the analysis. The nearest

strength of all other γ-rays of these nuclides were between 4 to 65 times lower than the

strongest γ-ray intensity. This property of the γ-rays of the above mentioned radioisotopes

facilitated the counting at the surface position without a significant loss in the net count

from the cascade or random summing. Additionally, the count rate in the whole spectrum

for all the ^{201}Tl counting were less than 100 sec^{-1} and for ^{68}Ge and ^{67}Ga radioisotopes it

was less than 20 sec^{-1}. The random summing effect, in most practical cases, is not

noticeable when the rate remains below 1000 sec^{-1} [24]. This is also verified by studying

the counting data of a standard source ^{57}Co at the surface and distant positions with

varying count rates from 92 to 1025 sec^{-1}. In another approach, 10 consecutively collected

net counts of ~10,000 of 122-keV line of ^{57}Co at the surface counting position with count

rate 92 sec^{-1}, were studied against the net counts of the same γ-ray collected introducing

different count rates up to 600 sec^{-1} using a standard ^{137}Cs source at various distances.

From these two exercises, it is concluded that random summing effects are insignificant

below a count rate of 100 sec^{-1}. The true coincident summing loss with the x-rays and

511–keV γ-rays resulting from the *EC* decay of ^{201}Tl and ^{67}Ga or *EC+β$^+$* decay of ^{68}Ge

was also studied. The HPGe detector was *p*-type having thicker window and thereby lower

efficiency for the x-rays and so summing loss with the x-rays were insignificant. A 15%

correction was applied to the ^{64}Zn(α,γ)^{68}Ge reaction cross section data for the summation

loss of the 1077–keV line with the 511–keV line. The correction factor was determined by

counting a ^{68}Ga source at 12–cm from the detector and at the surface positions. The source,

of about the same strength of the original sources, was produced bombarding a Zn sample

with 18–MeV α beams. The count rate for this ^{68}Ga source was 18 sec^{-1} at the detector

surface counting position, very similar to the original samples. Peak efficiency for the 1077–keV at 12–cm and surface positions were used for determining the correction factor. The surface peak efficiency was deduced normalizing the 25–cm efficiency data with the 835–keV single line from the [56]Mn standard source.

D. Thick-target yield calculation

The yields for the ^{64}Zn$(\alpha,\gamma)^{68}$Ge and ^{63}Cu$(\alpha,\gamma)^{67}$Ga reactions are calculated using equation (3) considering successive thin slices of 1000 angstrom (Å) thickness. The incident energy on each of these conceptual targets is obtained using *dE/dx* from the TRIM code [22]. The corresponding cross section is taken from a smooth fit made to the theoretical data from Ref. [21]. The consideration of conceptual target layers continued until the incident beam energy reached zero. The number of target nuclei, *n*, is calculated for the 1000 Å thickness using the Avogadro's number, elemental mass, and pure isotopic abundance in the target material. Finally, all thin target yields are summed to obtain the total calculated yield.

III. RESULTS AND DISCUSSION

Measured cross sections for the ^{197}Au$(\alpha,\gamma)^{201}$Tl, ^{197}Au$(\alpha,n)^{200}$Tl, and ^{197}Au$(\alpha,2n)^{199}$Tl reactions are presented in Table IV. The measured cross sections for the ^{197}Au$(\alpha,\gamma)^{201}$Tl reaction are presented in Fig. 2 along with the previously reported experimental [20] and theoretical data [21]. For determining the ^{197}Au$(\alpha,\gamma)^{201}$Tl cross section, the 167–keV γ–ray from ^{201}Tl is not observed in gold foils, bombarded with less than 17.9-MeV beam energy. Also the cross section at 18.6 MeV could not be extracted as that gold foil picked-up the radioisotope ^{51}Cr during irradiation from the closely spaced last target of titanium in the

stack. As a result, the weak 167–keV line was masked by the Compton continuum of the strong 320–keV line from [51]Cr.

TABLE IV. Measured cross sections (mb) of this experiment.

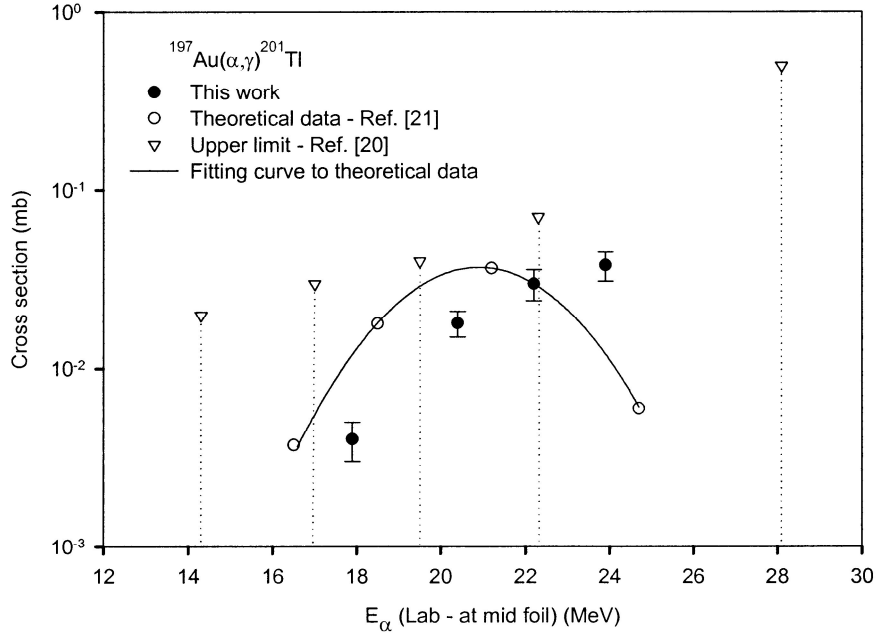| α-beam energy (MeV)	$^{197}Au(\alpha,\gamma)^{201}Tl$	$^{197}Au(\alpha,n)^{200}Tl$	$^{197}Au(\alpha,2n)^{199}Tl$
23.9 ± 0.2	0.038 ± 0.007	30 ± 5	562 ± 98
22.2 ± 0.4	0.030 ± 0.006	43 ± 6	332 ± 58
20.4 ± 0.4	0.018 ± 0.003	36 ± 5	71 ± 13
18.6 ± 0.4		7.2± 1.1	1.7 ± 0.4
17.9 ± 0.2	0.004 ± 0.001	5.5 ± 0.8	0.28 ± 0.07
15.8 ± 0.3		0.13± 0.02	
13.4 ± 0.3		0.05 ± 0.03	

FIG. 2. Cross sections for the $^{197}Au(\alpha,\gamma)^{201}Tl$ reaction.

From the measured γ–ray activities, the thick-target yield for the $^{64}Zn(\alpha,\gamma)^{68}Ge$ and $^{63}Cu(\alpha,\gamma)^{67}Ga$ reactions are deduced using equation (3) and corrected to pure isotopic targets using the natural abundance in the target material. The results are presented along

with the calculated thick-target yield in Table V as well as in Fig 3 for the $^{64}Zn(\alpha,\gamma)^{68}Ge$ reaction.

TABLE V. Measured and calculated thick-target yields for the $^{64}Zn(\alpha,\gamma)^{68}Ge$ and $^{63}Cu(\alpha,\gamma)^{67}Ga$ reactions.

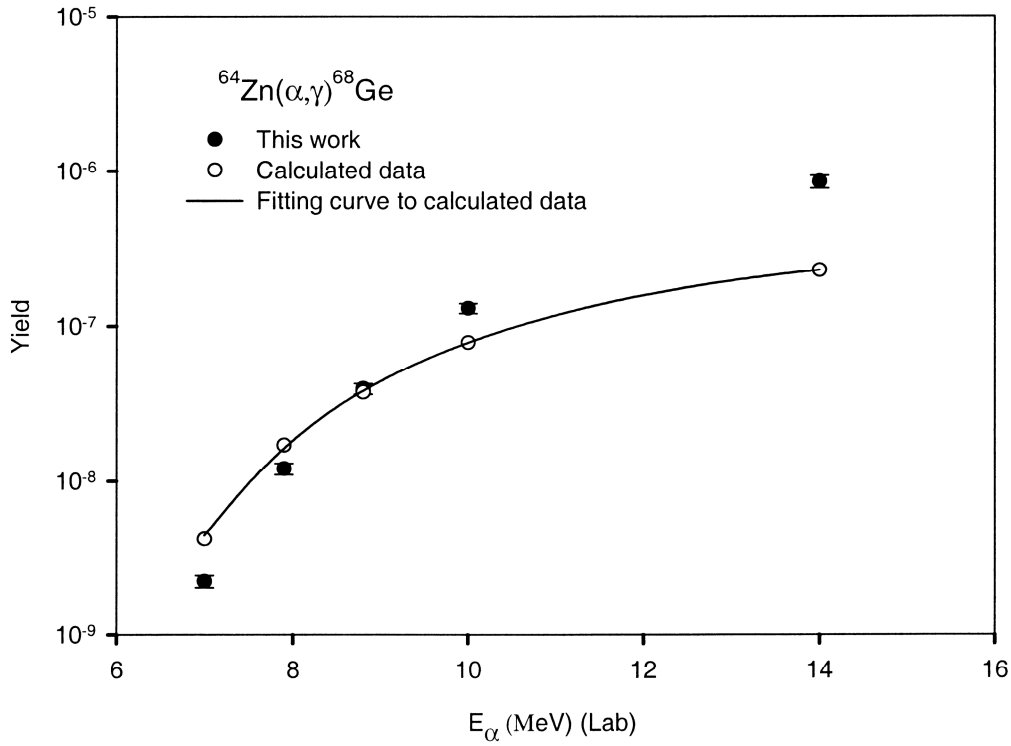| Nuclear Reaction	Beam energy (MeV)	Experimental yield	Calculated yield*
$^{64}Zn(\alpha,\gamma)^{68}Ge$	14.0 ± 0.2	$(8.5 \pm 0.8)E-7$	2.3E-7
	10.0 ± 0.1	$(1.3 \pm 0.1)E-7$	7.8E-8
	8.8 ± 0.1	$(3.9 \pm 0.3)E-8$	3.7E-8
	7.9 ± 0.1	$(1.2 \pm 0.1)E-8$	1.7E-8
	7.0 ± 0.1	$(2.2 \pm 0.2)E-9$	4.2E-9
$^{63}Cu(\alpha,\gamma)^{67}Ga$	7.0 ± 0.1	$(2.2 \pm 0.2)E-9$	3.2E-9

*Using energy dependent cross section data from Ref. [21].

FIG 3. Experimental and calculated yield for the $^{64}Zn(\alpha,\gamma)^{68}Ge$ reaction.

The $^{197}Au(\alpha,\gamma)^{201}Tl$ cross section in the energy range 17.9- to 23.9-MeV from this work reports the first consistent results for this nuclear reaction. As can be seen from Fig. 2, the

^{197}Au$(\alpha,\gamma)^{201}$Tl cross section data fall within the reported upper limits [20] and follow the theoretical values [21] in lower energy data points.

Cross section data for the ^{197}Au$(\alpha,n)^{200}$Tl and ^{197}Au$(\alpha,2n)^{199}$Tl reactions are reported in the literature at different energy ranges. The measured cross sections for these two reactions of this work are compared with the data of Ref. [25] and found to be consistent in the statistical limit considering the bombarding energy uncertainty of the incident beam.

Thick-target yields for the ^{64}Zn$(\alpha,\gamma)^{68}$Ge reaction are determined and compared with the calculated thick- target yields. As can be seen from Fig. 3, the experimental yield overlaps the calculated yield near the α-nucleus barrier height with an upward trend at higher energies and a lower trend at sub-barrier energies. The experimental energy dependent cross sections for the ^{63}Cu$(\alpha,\gamma)^{67}$Ga reaction reported earlier [10] were used for calculating the thick-target yield in the energy range 5.9- to 7.0-MeV. The resulting yield of 1.9×10^{-9} is consistent with the experimental value of the present work.

The alpha capture cross sections drop rapidly by several orders of magnitudes as the incident energy falls below the α-nucleus barrier height. As a result, cross section data at energies nearest to the bombarding energy contribute most highly to the total yield. So, a difference between the experimental and calculated thick-target yields basically indicates a qualitative difference between experiment and theory for the energy dependent cross section data near the bombarding energy. Thus, the study of the thick-target yield can provide useful information on the consistency between the experimental and theoretical energy dependent cross sections.

In an effort to provide experimental data in a wider target mass range for the scarcely available (α,γ) cross section data near or below the alpha-nucleus barrier interaction

energies, we report the cross sections and thick target yields in this work that follows our previous work for the $^{63}Cu(\alpha,\gamma)^{67}Ga$ reaction cross section [10]. From all these studies, it is observed that experimental data follow a trend of overlapping the predicted value near the alpha-nucleus barrier height and fall below with a slowly widening difference between them in the sub barrier energy points.

[1] S. E. Woosley and W. M. Howard, Astrophys. J. Suppl. **36**, 285 (1978).

[2] T. Rauscher, Phys. Rev. C **73**, 015804 (2006).

[3] T. Sauter and F. Kappeler, Phys. Rev. C **55**, 3127 (1997).

[4] J. Bork, H. Schatz, F. Käppeler, and T. Rauscher, Phys. Rev. C **58**, 524 (1998).

[5] F. R. Chloupek *et al.*, Nucl. Phys. **A652**, 391 (1999).

[6] E. Somorjai *et al.*, Nucl. Phys. **A621**, 293c (1997).

[7] Zs. Fülöp, Á. Z. Kiss, E. Somorjai, C. E. Rolfs, H-P. Trautvetter, T. Rauscher, and H. Oberhummer, Z. Phys. A **355**, 203 (1996).

[8] W. Rapp, M. Heil, D. Hentschel, F. Käppeler, and R. Reifarth, Phy. Rev. C **66**, 015803 (2002).

[9] N. Özkan *et al.*, Nucl. Phys. **A710**, 469 (2002).

[10] M. S. Basunia, E. B. Norman, H. A. Shugart, A. R. Smith, M. J. Dolinski, and B. J. Quiter, Phys. Rev. C **71**, 035801 (2005).

[11] P. Demetriou, C. Grama, and S. Goriely, Nucl. Phys. **A707**, 253 (2002).

[12] Gy. Gyürky, G. G. Kiss, Z. Elekes, Zs. Fülöp, E. Somorjai, A. Palumbo, J. Görres, H. Y. Lee, W. Rapp, M. Wiescher, N. Özkan, R. T. Güray, G. Efe, and T. Rauscher, Phys. Rev. C **74**, 025805 (2006).

[13] N. A. Roughton, M. R. Fritts, R. J. Peterson, C. S. Zaidins, and C. J. Hansen, At. Data Nucl. Data Tables **23**, 177 (1979).

[14] N. A. Roughton, T. P. Intrator, R. J. Peterson, C. S. Zaidins, and C. J. Hansen, At. Data Nucl. Data Tables **28**, 341 (1983).

[15] N. P. T. Bateman *et al.*, Phys. Rev. C **57**, 2022 (1998).

[16] C. M. Laymon, R. M. Prior, D. R. Tilley, and H. R. Weller, Phys. Rev. C **53**, 1977 (1996).

[17] J. D. Seagrave, Phys. Rev. **84**, 1219 (1951).

[18] E. B. Norman, T. E. Chupp, and K. T. Lesko, Astrophys. J. **251**, 834 (1981).

[19] F. K. McGowan, P. H. Stelson, and W. G. Smith, Phys. Rev. **133**, B907 (1964).

[20] C. Necheva and D. Kolev, Appl. Radiat. Isot. **48**, 807 (1997).

[21] T. Rauscher and F-K. Thielemann, At. Data Nucl. Data Tables **79,** 47 (2001). URL: http://quasar.physik.unibas.ch/~tommy/nosmo.html.

[22] J. F. Ziegler, J. P. Biersack, and U. Littmark, *The Stopping and Range of Ions in Solids* (New York, Pergamon Press, 1985).

[23] R. B. Firestone, and V. S. Shirley, *Table of Isotopes*, 8th Ed., (Wiley, New York, 1996).

[24] K. Debertin and R. G. Helmer, *Gamma- and X-ray Spectrometry with Semiconductor Detectors*, (Elsevier, New York, 1988).

[25] A. Calboreanu, C. Pencea, and O. Salagean, Nucl. Phys. **A383**, 251 (1982).